RICE UNIVERSITY

Search for Top Squark via All-Hadronic Decay Channels with Heavy Object Tagging

by

Matthew Cavenaugh Kilpatrick

A Thesis Submitted
in Partial Fulfillment of the
Requirements for the Degree

Doctor of Philosophy

Approved, Thesis Committee:

Karl Ecklund, Chair
Associate Professor of Physics and Astronomy

Paul Padley
Professor of Physics and Astronomy

David Scott
Noah Harding Professor

Houston, Texas

August, 2019

ABSTRACT

Search for Top Squark via All-Hadronic Decay Channels with Heavy Object Tagging

by

Matthew Cavenaugh Kilpatrick

Contents

Abstract ii

List of Figures vi

List of Tables vii

1 Introduction 1

1.1 Motivation 1

2 Supersymmetry and the Standard Model 2

2.1 The Standard Model 2

2.2 The Fundamental Particles 2

2.3 Quantum Field Theory 3

2.4 Noether's Theorem 4

2.5 Quantum Electrodynamics (QED) 4

2.6 Quantum Chromodynamics 6

2.7 Weak Force 8

2.8 The Electroweak Lagrangian 10

2.9 The Higgs Mechanism 11

2.10 Electroweak 13

2.10.1 The Standard Model Lagrangian 14

2.11 Fundamental Problems in the Standard Model 14

2.11.1 Dark Matter 15

2.11.2 Hierarchy Problem 15

2.11.3 Grand Unified Theory 17

2.12 Supersymmetry 18

2.12.1 Supermultiplets and Chirality 18
2.13 Minimal Supersymmetric Standard Model 19
2.13.1 R Parity 21
2.14 Mass Spectrums 21
2.15 Supersymmetry Searches 23

3 Compact Muon Solenoid 24
3.1 Introduction 24
3.2 Silicon Tracker 25
3.2.1 Pixel Detector 25
3.2.2 Silicon Strips 26
3.3 Electromagnetic Calorimeter 27
3.4 Hadronic Calorimeter 27
3.5 Superconducting solenoid 28
3.6 Muon Chambers 28
3.7 Physics Objects 30
3.8 Jets 30
3.9 Heavy Object Tagging 30

4 Stop quark Production and Backgrounds 32
4.1 Production and Decay Modes 32
4.2 Standard Model Background 32
4.2.1 Lost Lepton 32
4.2.2 Z Boson Decay to Neutrinos 33
4.2.3 Quantum Chromodynamic Events 33
4.2.4 Rare Interactions 33

5 Search Region Design 34
5.1 Minimizing the ttZ background 34

5.2 Lost Lepton Application 35
5.3 Search Regions 35
5.4 Search Region Optimization 35
5.5 Limits 35

Figures

2.1 The fundamental particles of the Standard Model. There are three generations of quarks and leptons. Along with the five bosons, where four of them relate to the interactions of the three forces included in the SM: Electromagnetism, the Weak force, and the Strong force and the final being the Higgs boson. 3
2.2 https://en.wikipedia.org/wiki/Cabibbo%E2%80%93Kobayashi%E2%80%93Maskawa_matr
2.3 Feynman diagram for Neutral Weak interaction 10
2.4 The loop corrections to the Higgs boson interacting with a top quark and its superpartner the top squark. This is a next-to-leading order (NLO) correction to the Higgs boson mass. 16
2.5 The energy dependence of the inverse gauge couple of each force in the SM (dashed line) and the MSSM (solid lines). The MSSM gives two thresholds for the sparticle mass 750 GeV and 2.5 TeV. 17
2.6 On the right we have the arbitrary masses of the top and charm quarks. 22

3.1 A cross-section of the CMS detector, oriented by looking down the direction of the beam pipe. 25
3.2 Geometry of the CMS Tracker, the inner most region in green in the pixel detector while the outer region in blue and red are the silicon strips. 26
3.3 A quarter cross-section of the three detection systems for CMS. . . . 29

Tables

2.1 Some words of explanation 5

2.2 The chiral supermultiplets of the MSSM. Spin-0 fields are complex scalars and spin-1/2 fields are left-handed two component Weyl fermions. CITE SUSY PRIMER 20

2.3 The chiral supermultiplets of the MSSM. CITE SUSY PRIMER . . . 20

Chapter 1

Introduction

1.1 Motivation

Chapter 2

Supersymmetry and the Standard Model

The fundamental theory of particle physics, known as the Standard Model (SM) can predict precise interactions between the fundamental particles in our universe. With these predictions we can confirm processes, but there are some aspects of the universe that have not yet been explained. In this Chapter, we will analyze the Standard Model, look at some specific shortcomings, and introduce supersymmetry as a possible solution.

2.1 The Standard Model

After decades of theoretical and experimental research the SM has been developed into a theory that explains the Electromagnetic (EM), Strong, and Weak forces. The SM has not yet been able to include Gravity within the theory. With the robust theoretical and experimental methods used in the SM, we have discovered new elementary particles and predicted others.

2.2 The Fundamental Particles

All matter can be explained by three kinds of elementary particles: leptons, quarks, and gauge bosons. Each of these can be distinguished by various quantum properties. The leptons and quarks are fermions, which are particles that have half-integer spin. Leptons are particles that only interact with the EM and Weak force, while quarks interact with all three forces of the SM. The gauge bosons are the force carries for each respective force and have integer spin.

There are three generations of leptons and quarks which are differentiated by a

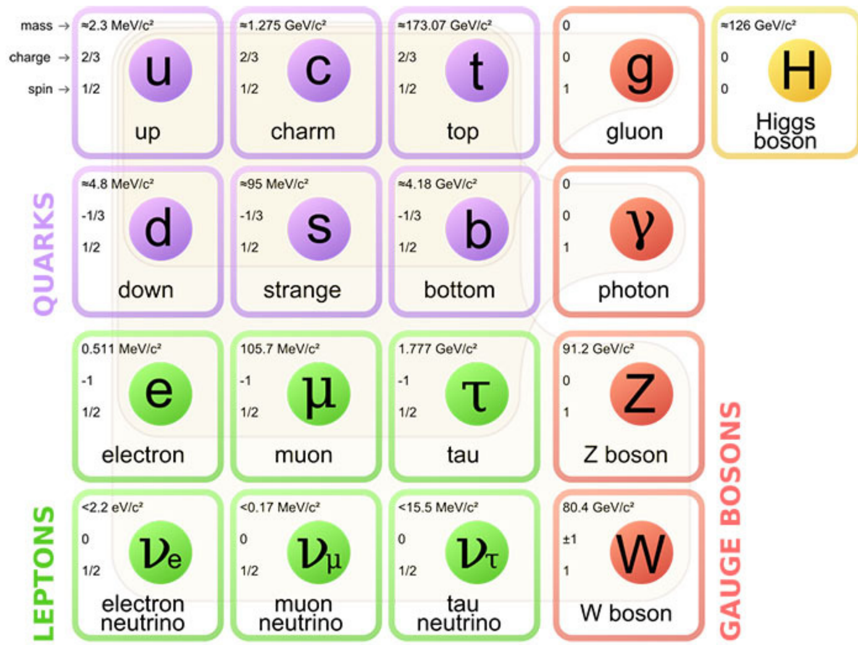

Figure 2.1 : The fundamental particles of the Standard Model. There are three generations of quarks and leptons. Along with the five bosons, where four of them relate to the interactions of the three forces included in the SM: Electromagnetism, the Weak force, and the Strong force and the final being the Higgs boson.

charge $\pm e$, the charge of an electron. Leptons have three different charged particles: electron (e), muon (μ), and tau (τ), with each charged particle having a corresponding neutrino (ν) of the same flavor, see fig 2.1. Quarks are also separated into three generations of doublets, the down-type ($-\frac{1}{3}e$): down (d), strange (s), and bottom (b) and up-type ($\frac{2}{3}e$): up (u), charm (c), and top (t), see fig 2.1. Each of the quarks has a color associated with it with is analogous to an electric charge, except there are three colors charges: red, blue, and green.

2.3 Quantum Field Theory

The interactions of all these particles are described by quantized fields whose operators describe the creation and annihilation of particles. Each of the fields of the SM have a corresponding gauge boson, see fig. 2.1. The most well-known being the

EM field and its interactions. In order to write a concise theory of the particles in the SM, the symmetry and conservation laws of the SM can be derived by starting with Noether's Theorem.

2.4 Noether's Theorem

Noether's theorem states,"to each symmetry of a local Lagrangian, there corresponds a conserved current". This can be done by allowing for an infinitesimal symmetry variation. Requiring the Lagrangian to be invariant under $\phi(x) \to \phi'(x) = \phi(x) + \alpha\Delta\phi(x)$, where α is infinitesimal real parameter and $\Delta\phi$ is a deformation to the field, up to a 4-divergance, the Lagrangian transforms as,

$$\mathcal{L}(x) \to \mathcal{L}(x) + \alpha\partial_\mu\mathcal{J}^\mu(x), \tag{2.1}$$

where $\mathcal{J}^\mu$ is a current. If we apply the Euler-Lagrange equation,

$$\partial_\mu(\frac{\partial\mathcal{L}}{\partial(\partial_\mu\phi)}) - \frac{\partial\mathcal{L}}{\partial\phi} = 0, \tag{2.2}$$

to Eqn. 2.1 with the addition of the fluctuation of the particle field. After some simplification we get a conserved current,

$$\begin{aligned} \partial_\mu j^\mu(x) &= 0, \text{ where} \\ j^\mu(x) &= \frac{\partial\mathcal{L}}{\partial(\partial_\mu\phi)}\Delta\phi - \mathcal{J}^\mu \end{aligned} \tag{2.3}$$

.

We see from the above equation that the current $j^\mu(x)$ of the Lagrangian is conserved. Now let's apply this to the particle fields of the SM.

2.5 Quantum Electrodynamics (QED)

First, we start with the assumption that the wave function $\psi(x)$ should transform as,

Type	Form	Components	Space Inversion
Scalar	$\overline{\psi}\psi$	1	$+$ under P
Vector	$\overline{\psi}\gamma^{\mu}\psi$	4	Space compts.: $-$ under P
Tensor	$\overline{\psi}\sigma^{\mu\nu}\psi$	6	
Axial Vector	$\overline{\psi}\gamma^{5}\gamma^{\mu}\psi$	4	Space compts.: $+$ under P
Pseudoscalar	$\overline{\psi}\gamma^{5}\psi$	1	$-$ under P

Table 2.1 : Some words of explanation

$$\psi(x) \rightarrow e^{i\alpha(x)}\psi(x), \tag{2.4}$$

where $\alpha(x)$ has an arbitrary dependence on space and time.

If one were to include this into the Lagrangian for a spin-1/2 particle in a vacuum,

$$\mathcal{L}_{QED}^{vac} = i\overline{\psi}\gamma^{\mu}\partial_{\mu}\psi - m\overline{\psi}\psi \tag{2.5}$$

where the γ^{μ} are the Dirac matrices, ∂_{μ} is the partial derivative, $\overline{\psi}$ is the hermitian conjugate of the wavefuntion ψ, and m is the mass of the particle. As a small aside, the bilinear quantities $\overline{\psi}(4\times4)\psi$ have certain properties under lorentz transformations when the 4×4 matix is a γ-matrices. These are of the form,

$$\gamma^0 = \begin{bmatrix} \boldsymbol{I} & 0 \\ 0 & -\boldsymbol{I} \end{bmatrix}, \boldsymbol{\gamma} = \begin{bmatrix} 0 & \boldsymbol{\sigma} \\ -\boldsymbol{\sigma} & 0 \end{bmatrix}, \gamma^5 = \begin{bmatrix} 0 & \boldsymbol{I} \\ \boldsymbol{I} & 0 \end{bmatrix} \tag{2.6}$$

where the $\boldsymbol{I}$ is the identity matrix and $\boldsymbol{\sigma}$ are the Dirac matrices. We can combine the first two parts of Eqn. 2.6 and write it compactly as γ^{μ} where $\mu = 0, 1, 2,$ and 3. The possible interesting quantities of the above transformations are shown in Table 2.1.

To allow for the field to be invariant, we must include a derivative, D_{μ}, that is covariant under phase transformations,

$$D_\mu \equiv \partial_\mu - ieA_\mu. \tag{2.7}$$

The covariant derivative includes the vector field A_μ which must also transform as,

$$A_\mu \to A_\mu + \frac{1}{e}\partial_\mu \alpha. \tag{2.8}$$

So after requiring that there be a local gauge transformation, we were forced to introduce a vector field A_μ, called the gauge field, which couples to Dirac particles in the same way as the photon field. We will think of this new field as the real photon field, which means we need to add a kinematic energy portion to the lagrangian. This kinematic term will be invariant under Eqn. 2.8, which leads us to final representation of the QED lagrangian which can be written down concisely as,

$$\mathcal{L}_{QED} = \overline{\psi}(i\gamma^\mu \partial_\mu - m)\psi + e\overline{\psi}\gamma^\mu A_\mu \psi - \frac{1}{4}F^{\mu\nu}F_{\mu\nu}, \tag{2.9}$$

where A_μ is the EM field operator and $F^{\mu\nu}$ is the EM field tensor. This Lagrangian describes the interactions between spin-1/2 charged particles and the $U(1)$ EM force. Each of the parts of this equation are lorentz invariant which allows this to be true in all reference frames.

2.6 Quantum Chromodynamics

Let's now transition from the description of the $U(1)$ EM field to the $SU(3)$ Quantum Chromodynamic (QCD) field and the transformation of quark fields. A quark in a vaccuum is described by,

$$\mathcal{L}^{vac}_{QCD} = \overline{q}_j(i\gamma^\mu \partial\mu - m)q_j, \tag{2.10}$$

where q_1, q_2, and q_3 are the three color fields. From this we want to require that the field is again invariant under another local phase transformation such as,

$$q(x) \to Uq(x) \equiv e^{i\alpha_a(x)T_a} q(x), \tag{2.11}$$

where U is a 3×3 unitary matix, T_a with $a = 1, \ldots, 8$ are a set of linearly independent traceless 3×3 matrices, and α_a are the group parameters. Since the generators T_a do not necessarily commute with each other, we can see that it is a non-Abelian transformation and the commutator can be represented as,

$$[T_a, T_b] = i f_{abc} T_c, \tag{2.12}$$

where f_{abc} are constants.

We need to impose $SU(3)$ local gauge invariance on Eqn. 2.10, to allow for the following phase transformations,

$$\begin{aligned} q(x) &\to (1 + i\alpha_a(x)T_a)q(x), \\ \partial_\mu q &\to (1 + i\alpha_a T_a)\partial_\mu q + iT_a q \partial_\mu \alpha_a. \end{aligned} \tag{2.13}$$

From this is seems straight forward that we can proceed in exactly the same manner as QED, which is to add a transformation to the derivative,

$$D_\mu = \partial_\mu + i g_Q T_a G^a_\mu. \tag{2.14}$$

where the field G^a_μ transforms as,

$$G^a_\mu \to G^a_\mu - \frac{1}{g_Q}\partial_\mu \alpha_a, \tag{2.15}$$

where g_Q is the coupling strength of QCD interactions. This will give us a similar Lagrangian to the QED one derived above, but this is not sufficient for a non-Abelian gauge transformation and it does not produce a gauge-invariant Lagrangian. One final transformation is required for the G^a_μ fields,

$$G^a_\mu \to G^a_\mu - \frac{1}{g_Q}\partial_\mu \alpha_a - f_{abc}\alpha_b G^c_\mu. \tag{2.16}$$

This finally gives us a gauge invariant kinetic energy term for all the G^a_μ fields and thus we can write the QCD interactions as,

$$\mathcal{L}_{QCD} = \overline{q}(i\gamma^\mu \partial_\mu - m)q - g_Q(\overline{q}\gamma^\mu T_a q)G^a_\mu - \frac{1}{4}G^a_{\mu\nu}G^{\mu\nu}_a. \tag{2.17}$$

From all of this we seem to be missing a vital part of the SM, specifically a theory for the Weakly interacting processes which is mediated by the massive bosons, W and Z from fig. 2.1.

2.7 Weak Force

The Weak force is responsible for nuclear decay. The Weak force has an interaction of the type $\frac{1}{2}\gamma^\mu(1-\gamma^5)$ so it is a V-A interaction with $SU(2)$ symmetry. From this, we can conclude that it violates Parity. Parity is a transformation from $(x, y, z) \to (-x, -y, -z)$ or space inversion. Since it violates Parity, the next step is to consider a conservation of CP, where C is charge conjugation (particle-to-antiparticle).

The main experimental implications of this proposed conservation comes from the decay of the neutral Kaon, $K^0(\overline{s}d)$ and $\overline{K}^0(s\overline{d})$. These have two CP states which are, $CP\,|K^0\rangle = -\,|\overline{K}^0\rangle$, and $CP\,|\overline{K}^0\rangle = -\,|K^0\rangle$. Once we normalize these eigenstates of CP we get the corresponding wavefunctions,

$$|K_1\rangle = \left(\frac{1}{\sqrt{2}}\right)(|K^0\rangle - |\overline{K}^0\rangle) \text{ and } |K_2\rangle = \left(\frac{1}{\sqrt{2}}\right)(|K^0\rangle + |\overline{K}^0\rangle),$$

where each has the invariance $CP\,|K_1\rangle = |K_1\rangle$ and $CP\,|K_2\rangle = -\,|K_2\rangle$. The two Kaon states are expected to decay into either two pions or three pions for $|K_1\rangle$ and $|K_2\rangle$, respectively. Since there is a greater energy release in the $|K_1\rangle$ state the lifetime of that particle is thought to be less than $|K_2\rangle$. After experimenting on the purity of Kaon decays after a long distance away from an interaction point, we have found that it is possible for the $|K_1\rangle$ to decay into three pions. This is direct evidence of Weak decays violating CP conservation.

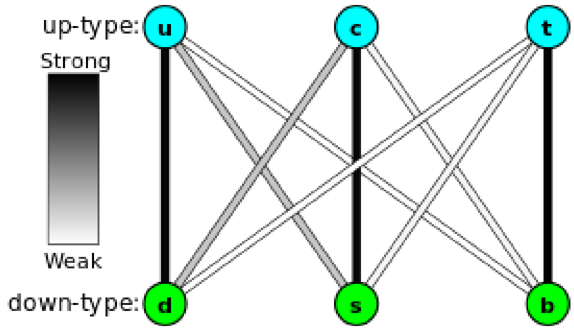

Figure 2.2 : https://en.wikipedia.org/wiki/Cabibbo%E2%80%93Kobayashi%E2%80%93Maskawa_m

Now the Weak force is mediated by two vector bosons, W and Z , see fig. 2.1. These are unlike the other forces because these vector bosons have a large mass of $m_W = 80.379 \pm 0.012$ GeV and $m_Z = 91.1876 \pm 0.0021$ GeV. The W boson is a charged particle and interacts with many nuclear decays.

The W boson interacts very interestingly for quarks in the SM. There is a mixing of flavors of quarks for particles. They will mix partners between up-type and down-type particles, see fig. 2.2. [Kobayashi, M. and Maskawa, K. (1973) Progress in Theoretical Physics, 49, 652]. The interactions for the generalized three generations of quarks is known as the Cabibbo-Kobayashi-Maskawa (CKM) matrix,

$$\begin{bmatrix} d' \\ s' \\ b' \end{bmatrix} = \begin{bmatrix} V_{ud} & V_{us} & V_{ub} \\ V_{cd} & V_{cs} & V_{cb} \\ V_{td} & V_{ts} & V_{tb} \end{bmatrix} \begin{bmatrix} d \\ s \\ b \end{bmatrix}, \tag{2.18}$$

where for example, V_{ud} is the coupling of u to d which is exactly $(d \to u + W^-)$. This matrix can be reduced to a form which has three generalized Cabibbo angles $(\theta_{12}, \theta_{23}, \theta_{13})$ and a phase factor (δ). The coupling between the third generation does not mix with the other two generations. From that we can recover the Cabibbo-GIM matrix[cite here]. For the moment, we can only determine these values from experimentation.

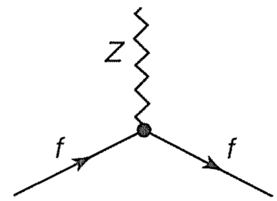

Figure 2.3 : Feynman diagram for Neutral Weak interaction

The Z boson is known as the neutral current. This boson mediates forces between particles and their respective antiparticles, see fig. 2.3. This interaction for the neutral weak force is $\gamma^\mu(c_V^f - c_A^f\gamma^5)$ which is quite similar to the charged weak interaction, but differs by the constants c_V^f and c_A^f.

2.8 The Electroweak Lagrangian

The simplest group for the Electroweak interaction is $SU(2)_L \times U(1)_Y$ which will give the left-handed interactions in doublets with the addition of massive gauge bosons W and Z with a massless photon. We first consider the free Lagrangian,

$$\mathcal{L} = \overline{\psi}_j\gamma^\mu\psi_j, \tag{2.19}$$

where j is the fermion wavefunction. We are not including the mass parameter because it would cause the left and right-handed parts to mix. This is assumed to transform under the global invariant

$$\begin{aligned} \chi_L \rightarrow \chi_L' &= e^{i\frac{\tau_a}{2}\alpha^a(x)+i\beta(x)Y}\chi_L, \\ \psi_R \rightarrow \psi_R' &= e^{i\beta(x)Y}\psi_R \end{aligned} \tag{2.20}$$

where the transformation $e^{i\frac{\tau_a}{2}\alpha^a(x)}$ with $a = 1, 2, 3$ is the $SU(2)_L$ transformation and only acts on the left-handed doublet. The next step is to require that the Lagrangian is invariant under local $SU(2)_L \times U(1)_Y$. We allow for the following covariant derivatives,

$$\begin{aligned} D_\mu \psi_1 &= [\partial_\mu - i g_W \frac{\tau_a}{2} W^a_\mu - i g'_W y_1 B_\mu]\psi_1 \\ D_\mu \psi_2 &= [\partial_\mu - i g'_W y_2 B_\mu]\psi_2 \\ D_\mu \psi_3 &= [\partial_\mu - i g'_W y_3 B_\mu]\psi_3 \end{aligned} \tag{2.21}$$

where g_W and g'_W are the Weak force coupling constants while W^a_μ and B_μ are four gauge bosons and can be the possible candidates for $W^\pm$, Z and γ. Just like the above derivations the fields need to transform along with the wavefuntions and derivatives. These transformations are,

$$\begin{aligned} B_\mu \rightarrow & B'_\mu = B_\mu + \frac{1}{g'_W}\partial_\mu \beta(x) \\ W\mu \rightarrow & W'_\mu = U_L W_\mu U_L^\dagger - \frac{1}{g_W}\partial_\mu U_L U_L^\dagger \end{aligned} \tag{2.22}$$

where $U_L = e^{i\frac{\tau_a}{2}\alpha^a(x)}$. These transformation are similar to the QED and QCD transformation. If we include all of these invariant transformations in the free Weak Lagrangian Eqn. 2.19 and we get a free invariant Lagrangian, but this does not allow us to include a mass term for the fermions. Therefore this is not a viable procedure to include the Electroweak interactions into the model. In order to do this we must include the Higgs Mechanism.

2.9 The Higgs Mechanism

We are interested in the spontaneous symmetry breaking of a local $SU(2)$ gauge symmetry. Specifically, the following Lagrangian,

$$\mathcal{L} = (\partial_\mu \phi)^\dagger (\partial^\mu \phi) - \mu^2 \phi^\dagger \phi - \lambda(\phi^\dagger \phi)^2, \tag{2.23}$$

with ϕ being a $SU(2)$ doublet of complex scalar fields,

$$\phi = \frac{1}{2}\begin{bmatrix}\phi_1 + i\phi_2 \\ \phi_3 + i\phi_4\end{bmatrix} \tag{2.24}$$

and is invariant under global $SU(2)$ phase transformations $\phi \rightarrow e^{i\alpha_a \tau_a/2}\phi$. To allow for local invariance, we first allow for a covariant derivative,

$$D_\mu = \partial_\mu + ig_W \frac{\tau_a}{2} W_\mu^a, \tag{2.25}$$

where we now have three gauge fields, W_μ^a. If we assume an infanitesimal gauge transformation for the $SU(2)$ doublet $\phi(x) \rightarrow \phi'(x) = (1 + i\frac{\tau_a}{2}\alpha^a(x))\phi(x)$, then the gauge fields will transform as,

$$W_\mu^a \rightarrow W_\mu^a - \frac{1}{g_W}\partial_\mu \alpha_a - f_{abc}\alpha_b W_\mu^c. \tag{2.26}$$

You can see that Eqn. 2.26 is just the compact vector transform of Eqn. 2.16 where we have replaced the QCD gauge field with the three gauge fields W_μ^a. If we include these locally invariant transformations into the above $SU(2)$ Lagrangian we get,

$$\mathcal{L} = (\partial_\mu \phi + ig_W \frac{1}{2}\tau_a W_\mu^a \phi)^\dagger (\partial^\mu \phi + ig_W \frac{1}{2}\tau_a W^{a\mu}\phi) - \mu^2 \phi^\dagger \phi + \lambda(\phi^\dagger \phi)^2 - \frac{1}{4}W_{\mu\nu}^a W^{a\mu\nu}, \tag{2.27}$$

where the gauge field kinetic term has been included at the end. The most interesting regions of this Lagrangian is when $\mu^2 < 0$ and $\lambda > 0$, and the potential has a minimum at $\phi^\dagger \phi = -\frac{\mu^2}{2\lambda}$. With this we will expand the potential around the minimum and require that,

$$\phi_1 = \phi_2 = \phi_4 = 0, \phi_3^2 = -\frac{\mu^2}{2\lambda} \equiv v^2. \tag{2.28}$$

This is the spontaneous symmetry breaking of the $SU(2)$ symmetry, because of this we are able to substitute an expansion for the field,

$$\phi = \sqrt{\frac{1}{2}} \begin{bmatrix} 0 \\ v + h(x) \end{bmatrix} \tag{2.29}$$

With this specific transformation of the $SU(2)$ doublet and the simplification of Eqn. 2.27, the only remaining field is $h(x)$ which is refered to as the Higgs field. This is what is known as the Higgs Mechanism for a $SU(2)$ symmetry.

2.10 Electroweak

We want to include the Higgs Mechanism into the Weak isospin and Weak hypercharge,$SU(2)_L \times U(1)_Y$, transformations of electoweak interactions. First, we need to include the coupling of the Weak current J^a_μ and the gauge field $W^{a\mu}$ such that,

$$-ig_W J^a_\mu W^{a\mu} = -ig_W \overline{\chi}_L \gamma_\mu T^a W^{a\mu} \chi_L \tag{2.30}$$

which is the basic interaction for the $SU(2)_L$ symmetry. Then, we also need to include the weak hypercharge current with the fourth vector boson B^μ,

$$-i\frac{g'_W}{2} j^Y_\mu B^\mu = -ig'_W \overline{\psi} \gamma_\mu \frac{Y}{2} \psi B^\mu, \tag{2.31}$$

here the operators T^a and Y are generators for the $SU(2)_L$ and $U(1)_Y$ gauge transformations, respectively. Now we combine the two symmetries with the transformations of the left and right hand components of ψ and from this we can write down the contributions of the two gauge fields W^3_μ and B_μ and the mising angle θ_W to find the interactions of the two neutral currents. The physical fields are thus,

$$-ig_W J^3_\mu W^{3\mu} - i\frac{g'_W}{2} j^Y_\mu B^\mu = -iej^{em}_\mu A^\mu - \frac{ie}{sin\theta_W cos\theta_W}[J^3_\mu - sin^2\theta_W j^{em}_\mu] Z^\mu. \tag{2.32}$$

From this we can write down the Electroweak Lagrangian, for any fermion that interacts with the field. Moreover, we can formulate the Higgs mechanism, such that we can calculate the theoretical masses of the gauge bosons and fermions as,

$$
\begin{aligned}
M_W &= \frac{1}{2} v g_W \\
M_Z &= \frac{1}{2} v \sqrt{g_W^2 + g_W'^2},
\end{aligned} \tag{2.33}
$$

but these masses cannot be predicted since they depend on the values from the chosen Higgs field.

2.10.1 The Standard Model Lagrangian

With the inclusion of the Higgs mechanism and the formulation of a local gauge invariant Lagrangian for the Electroweak and QCD fields, we have the complete SM Lagrangian as,

$$
\begin{aligned}
\mathcal{L} = &- \frac{1}{4} W^a_{\mu\nu} W^{a\mu\nu} - \frac{1}{4} B_{\mu\nu} B^{\mu\nu} - \frac{1}{4} G^a_{\mu\nu} G^{\mu\nu}_a \\
&+ \overline{L} \gamma^\mu (i\partial_\mu - g_W \frac{1}{2} \tau^a W^a_\mu - g'_W \frac{Y}{2} B_\mu - g_Q T_b G^b_\mu) L \\
&+ \overline{R} \gamma^\mu (i\partial_\mu - g'_W \frac{Y}{2} B_\mu - g_Q T_b G^b_\mu) R \\
&+ |(i\partial_\mu - g_W \frac{1}{2} \tau^a W^a_\mu - g'_W \frac{Y}{2} B_\mu) \phi|^2 - V(\phi) \\
&- (G_1 \overline{L} \phi R + G_2 \overline{L} \phi_c R + \text{hermitian conjugate}),
\end{aligned} \tag{2.34}
$$

where the first terms are the kinetic energies and self-interactions of the $W^\pm, Z, g,$ and γ bosons, the second and third terms are the kinetic energies and interactions of the leptons and quarks with the $W^\pm, Z, g,$ and γ bosons where L is a left-handed fermion doublet and R is a right-handed fermion singlet. The fourth term is the $W^\pm, Z, \gamma$ and Higgs masses and couplings. The final term is the lepton and quark masses and couplings to the Higgs field.

2.11 Fundamental Problems in the Standard Model

The SM is able to accurately and precisely describe many facets of the universe. Whether it comes to predicting the existence of a sixth quark or the confirmation of

$g-2$ for the muon to 9 orders of magnitude. Unfortunately, there is some evidence of matter or interactions that cannot be described such as dark matter, the Hierarchy problem, and a possible grand unified theory. Let's look into each of these further.

2.11.1 Dark Matter

The main motivation for Dark Matter is the difference between the visible matter and the measureable matter in the universe. This has most notably been seen in the radial velocities of stars in galaxies. In a galaxy which is solely made up of visible matter, matter that interacts with light, the radial velocity of stars should decrease as $1/\sqrt{r}$ the further away it is from the galactic nuclei, although measurements show the velocity becoming constant as a function of radius.

The original study of this was from the galaxy NGC 1560, where the measured galactic velocity curve provided a result that was 400 times large than the visible matter in the cluster (A. H. Broeils Astron. and Astrophys. 256 19 (1992)). To reproduce these features in models, the mass of the galaxy must be significantly more than what is seen. This implies some unseen dark matter, that still interacts with the gravitational field but not with the EM field. There is currently no such particle in the SM that has these properties.

2.11.2 Hierarchy Problem

The Higgs boson is a beautiful solution to electroweak symmetry breaking and gives a method for particles to acquire mass, see Sec. 2.9, and was discovered to have a measured mass of $m_H = 125.18 \pm 0.16$ GeV. This value though is not predictable with the SM and leads to some inconsistencies when you include loop corrections. Since the Higgs is strongly coupled to particles with large masses, the dominant loop correction is due to interactions with the t quark. These higher order loop corrections to the Higgs mass, m_H^2, caused by the fermionic t loop, see fig 2.4, are,

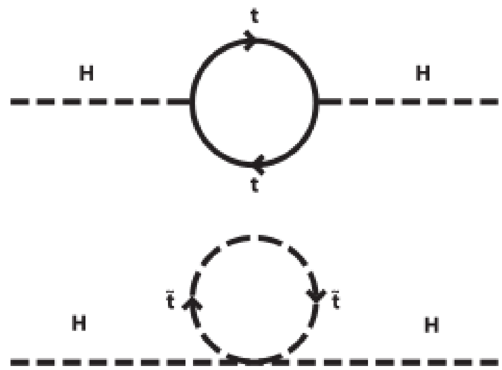

Figure 2.4 : The loop corrections to the Higgs boson interacting with a top quark and its superpartner the top squark. This is a next-to-leading order (NLO) correction to the Higgs boson mass.

$$\Delta m_H^2 = -\frac{|\lambda_f|^2}{8\pi^2}\Lambda_{UV}^2 + \cdots, \tag{2.35}$$

where λ_f is the vertex factor for the respective fermion and Λ_{UV} is the ultraviolet momentum cutoff. The Higgs boson loop corrections are highly dependent on all virtual and real particles that couple to the Higgs field. From this, we can see the corrections from Eqn. 2.35 for each fermion in the SM will cause a large divergence. The quadratic divergence of the Higgs mass is only renormalizable with a fine tuning of the parameters λ_f and Λ_{UV}. This means the only way for the SM to reconcile this unfortunate fact is to have a relatively lucky cancellation of very large numbers of order 10^{32} with equally small numbers. Fortunately, if we add the contribution of a bosonic partner of the fermion the Higgs loop corrections reduce to,

$$\Delta m_H^2 = \frac{\lambda_S}{16\pi^2}[\Lambda_{UV}^2 - 2m_S^2 ln(\Lambda_{UV}/m_S) + \cdots]. \tag{2.36}$$

With the introduction of a scalar partner to the t, there is a logarithmic divergence to the higgs boson mass and can be renormalized through the normal methods.

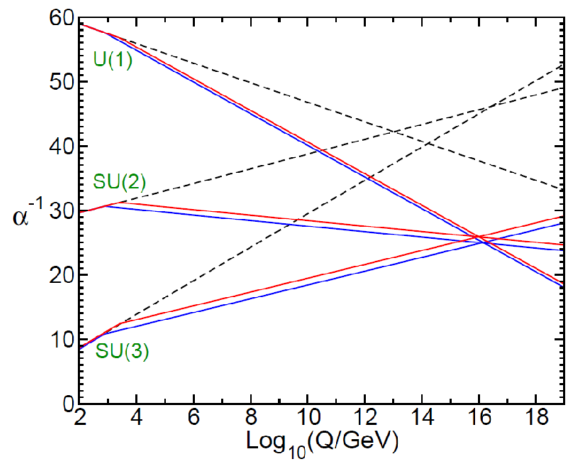

Figure 2.5 : The energy dependence of the inverse gauge couple of each force in the SM (dashed line) and the MSSM (solid lines). The MSSM gives two thresholds for the sparticle mass 750 GeV and 2.5 TeV.

2.11.3 Grand Unified Theory

The SM is able to accurately describe three of the fundamental sources at typical energy scales, 1 to 10^4 GeV, but idealy the forces would be able to merge into a single force at higher energies. This has not been directly observed, but many theories, such as supersymmetry (SUSY), predict its existence.

At standard energies for particle physics experiments the difference in the strength of each force is quite noticeable. But it has been shown that in the SM the strengths of each force are dependent on the energy scale and it would be ideal that they converge to a single force at large energies, such as 10^{16} GeV. In fig. 2.5, we see the extrapolated energy scales of the forces in the SM shown as the dotted line. These unfortunately, do not meet at a single point to become one force, but if we include supersymmetry into the model we get a nice convergence between the forces.

2.12 Supersymmetry

We have seen from the above three problems that there is still more to learn. Some of the features of the universe, such as; dark matter, the hierarchy problem, and a grand unified theory have not been explained. We saw from the Hierarchy problem that the addition of a bosonic partner to a fermion will allow for the loop corrections to be renormalizable without fine tuning. Fortunately, some theories have allowed for such a problem to be solved. Namely the theory of SUSY which essentially states that each particle in the SM has a superpartner that has only the spin changed, that every fermion has a bosonic partner that has all the same quantum numbers except the spins differ by 1/2, and vice-versa.

The partners to the fermions are denoted with a 's' in front of the name to notify that it is the scalar form of the particle and the partners to the bosons have an 'ino' attached at the end, such as photino, gluino, wino, and Higgsino. So for the partners to the fermionic particles in the standard model we have: sup ($\widetilde{u}$), sdown ($\widetilde{d}$), scharm ($\widetilde{c}$), sstrange ($\widetilde{s}$), stop ($\widetilde{t}$), and sbottom ($\widetilde{b}$) for the squarks and selectron ($\widetilde{e}$), smuon ($\widetilde{\mu}$), and stau ($\widetilde{\tau}$) for the charged sleptons. The partners to the neutrinos, which are always left-handed if you neglect the minimal masses, are sneutrinos ($\widetilde{\nu}_e, \widetilde{\nu}_\mu, \widetilde{\nu}_\tau$), where whe have one for each flavor of lepton.

If the SUSY was unbroken the superpartners would have exactly the same properties as the SM pairs except their spin. This would cause a massless photino or a $m_{\widetilde{e}} = 0.511$ keV selectron. These particles would certainly have been detected at this point, which leads us to think that SUSY is a broken symmetry where all the superpartners have a mass that is significantly higher than their SM partners.

2.12.1 Supermultiplets and Chirality

A supermultiplets is any symmetry where the number of bosonic degrees of freedom and fermionic degrees of freedom are equal, $n_B = n_F$. The simplest way to achieve this is to have a combination of a single Weyl fermion, which is a chiral representation of the fermion and has two spin helicity states, $n_F = 2$, and two real scalars with each having $n_B = 1$. It becomes convenient for the mathematics to combine the two real scalars into one complex scalar field. Now the combination of a complex scalar field and a Weyl fermion is known as a chiral supermultiplet.

2.13 Minimal Supersymmetric Standard Model

We have discussed how the fermions transform under the rules of SUSY, but how do the scalar field mediators translate into this new framework. First, lets look at the Higgs boson. We know that there is not only one chiral supermultiplets. If there was only one in the electroweak gauge symmetry, with a Higgsino of spin-1/2, would not have the anomaly cancellation of the traces, $Tr[T_3^2 Y] \neq 0$ and $Tr[Y^3] \neq 0$, where T_3 is the third component of weak isospin and Y is the weak hypercharge. In the SM, the traces of these for the fermions are already satified. So we must include two chiral supermultiplets of the Higgsino, with $Y = \pm\frac{1}{2}$, see table 2.2.

It turns out that this is also necessary for the Higgsino to give mass to different particles in the SM. A Higgs boson with $Y = 1/2$ has the Yukawa couplings that allow it to interact with the up-type quarks (u, c, t). Only a Higgs boson with $Y = -1/2$ has the correct Yukawa couplings to interact with the down-type quarks (d, s, b) and the charged leptons (e, μ, τ).

The SM vector boson will also have a corresponding chiral supermultiplet. They have fermionic superpartners that are referred to as gauginos. For the $SU(3)_C$ color gauge interactions of QCD, which are a spin-1/2 color-octet, has a partner called a gluino $(\widetilde{g})$. The electroweak gauge theory $SU(2)_L \times U(1)_Y$ has the superpartners $\widetilde{W}^+, \widetilde{W}^0, \widetilde{W}^-,$ and $\widetilde{B}^0$ each with spin-1/2, called winos and bino, see table 2.3. The gaugino mixtures of $\widetilde{W}^0$ and $\widetilde{B}^0$ give the corresponding zino $(\widetilde{Z}^0)$ and photino $(\widetilde{\gamma})$. The chiral supermultiplets shown in table 2.2 and 2.3 give the particles of the Minimal Supersymmetric Standard Model (MSSM).

Names		spin 0	spin 1/2	$SU(3)_C$, $SU(2)_L$, $U(1)_Y$
squarks, quarks	Q	$(\widetilde{u}_L \;\; \widetilde{d}_L)$	$(u_L \;\; d_L)$	$(\,\mathbf{3},\, \mathbf{2}\,,\, \frac{1}{6})$
(×3 families)	$\overline{u}$	$\widetilde{u}^*_R$	$u^\dagger_R$	$(\,\overline{\mathbf{3}},\, \mathbf{1},\, -\frac{2}{3})$
	$\overline{d}$	$\widetilde{d}^*_R$	$d^\dagger_R$	$(\,\overline{\mathbf{3}},\, \mathbf{1},\, \frac{1}{3})$
sleptons, leptons	L	$(\widetilde{\nu}\;\widetilde{e}_L)$	$(\nu \;\; e_L)$	$(\,\mathbf{1},\, \mathbf{2}\,,\, -\frac{1}{2})$
(×3 families)	$\overline{e}$	$\widetilde{e}^*_R$	$e^\dagger_R$	$(\,\mathbf{1},\, \mathbf{1},\, 1)$
Higgs, higgsinos	H_u	$(H_u^+ \;\; H_u^0)$	$(\widetilde{H}_u^+ \;\; \widetilde{H}_u^0)$	$(\,\mathbf{1},\, \mathbf{2}\,,\, +\frac{1}{2})$
	H_d	$(H_d^0 \;\; H_d^-)$	$(\widetilde{H}_d^0 \;\; \widetilde{H}_d^-)$	$(\,\mathbf{1},\, \mathbf{2}\,,\, -\frac{1}{2})$

Table 2.2 : The chiral supermultiplets of the MSSM. Spin-0 fields are complex scalars and spin-1/2 fields are left-handed two component Weyl fermions. CITE SUSY PRIMER

Names	spin 1/2	spin 1	$SU(3)_C$, $SU(2)_L$, $U(1)_Y$
gluino, gluon	$\widetilde{g}$	g	$(\,\mathbf{8},\, \mathbf{1}\,,\, 0)$
winos, W bosons	$\widetilde{W}^\pm \;\; \widetilde{W}^0$	$W^\pm \;\; W^0$	$(\,\mathbf{1},\, \mathbf{3}\,,\, 0)$
bino, B boson	$\widetilde{B}^0$	B^0	$(\,\mathbf{1},\, \mathbf{1}\,,\, 0)$

Table 2.3 : The chiral supermultiplets of the MSSM. CITE SUSY PRIMER

2.13.1 R Parity

R-parity or matter parity is the multiplicatively conserved quantum number defined as,

$$P_R = (-1)^{3(B-L)+2s}, \tag{2.37}$$

where B is the baryon number, L is the lepton number, and s is the spin of the particle. From this we can find the R-parity of all the particles in the SM and MSSM. The definition of R-parity is quite useful because all the particles of the SM have an R-partity of $P_R = +1$, while all of the squarks, sleptons, gauginos, and higgsinos have $P_R = -1$.

R-parity is thought to be exactly conserved in SUSY, where there is no mixing between particles ($P_R = +1$) and sparticles ($P_R = -1$). This leads to three important consequences:

- The lightest sparticle that has $P_R = -1$ is called the "lightest supersymmetric particle" or LSP, which must be absolutely stable. If it is electrically neutral, it is a possible non-baryonic dark matter candidate.
- Every sparticle, other than the LSP, must eventually decay into an odd number of LSPs.
- For collider experiments, sparticles will only be produced in even numbers.

We are going to be investigating a MSSM that conserves R-parity. This is quite well motivated by the possiblilty of a dark matter candidate and putting constraints on proton decay.

2.14 Mass Spectrums

The third family of squarks and sleptons should have quite different masses compared to their first- and second-family counterparts, which is caused by the large

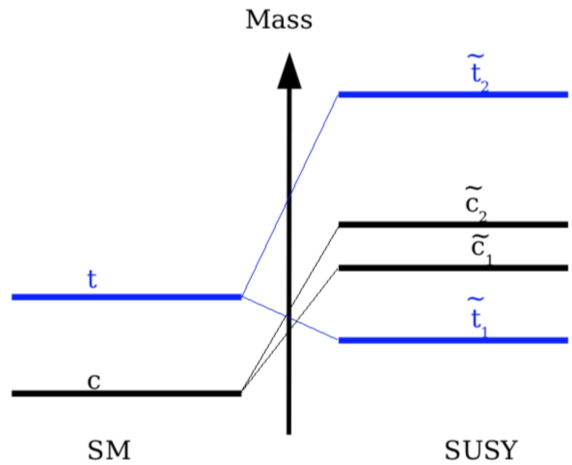

Figure 2.6 : On the right we have the arbitrary masses of the top and charm quarks.

Yukawa (y_t, y_b, y_τ) and soft (a_t, a_b, a_τ) couplings. This causes significant mixing between the chiral superpartners $(\widetilde{t}_L, \widetilde{t}_R), (\widetilde{b}_L.\widetilde{b}_R)$, and $(\widetilde{\tau}_L, \widetilde{\tau}_R)$. We will concentrate on how the mass of the top squark, $\widetilde{t}$ evolves in the MSSM. Given many contributions to the top squark mass such as; squared-mass terms, 4-vertex interactions terms with the up-type Higgs, the 3-vertex interactions with the down-type Higgs, and scalar potential couplings. Accounting for all these contributions, we have a square-mass matrix for the top squarks,

$$\mathcal{L}_{\text{stop masses}} = -\begin{bmatrix} \widetilde{t}_L^* & \widetilde{t}_R^* \end{bmatrix} \boldsymbol{m}^{\boldsymbol{2}}_{\boldsymbol{\widetilde{t}}} \begin{bmatrix} \widetilde{t}_L \\ \widetilde{t}_R \end{bmatrix} \tag{2.38}$$

where

$$\boldsymbol{m}^{\boldsymbol{2}}_{\boldsymbol{\widetilde{t}}} = \begin{bmatrix} m^2_{Q_3} + m_t^2 + (\frac{1}{2} - \frac{2}{3} sin^2\theta_W) cos(2\beta) m_Z^2 & v(a_t^* sin\beta - \mu y_t cos\beta) \\ v(a_t sin\beta - \mu^* y_t cos\beta) & m^2_{\overline{u}_3} + m_t^2 + (\frac{2}{3} sin^2\theta_W) cos(2\beta) m_Z^2 \end{bmatrix}. \tag{2.39}$$

This is a hermitian matrix and can be diagonalized to give eigenstates $\widetilde{t}_1$ and $\widetilde{t}_2$ which are linear combinations of the left and right-handed $\widetilde{t}$, see fig. 2.6. Now we get the eigenvalues for the mass states as $m^2_{\widetilde{t}_1} < m^2_{\widetilde{t}_2}$. From this models predict that the $\widetilde{t}_1$ is the lightest squark.

2.15 Supersymmetry Searches

The SM of particle physics has been a powerful model for predicting interactions between quarks, leptons, and force carriers, with an accurate prediction for precision measurements, but has some faults such as, the Hierarchy problem, dark matter, and a Grand Unified Theory. We have seen that including SUSY can allow for possible solutions, such as: a dark matter candidate as the LSP, bosonic-fermionic loop corrections for the Higgs boson mass, and a unification of the fundamental forces at large energies. Then once investigating the theory of SUSY we were able to determine that the top squark would be the light squark, which allows us to develop multiple searches for this proposed theory.

Chapter 3

Compact Muon Solenoid

3.1 Introduction

The Compact Muon Solenoid (CMS) is a particle detector as part of the Large Hadron Collider (LHC) which is located near Geneva, Switzerland as part of the CERN collaboration. The CMS detector is 21.6 m long, 15 m diameter, and 14,000 tons and is used to detect many different species of particles. It is separated into layers that, from the interaction vertex outward are, the silicon tracker, Electromagnetic Calorimeter (ECAL), Hadronic Calorimeter (HCAL), superconducting solenoid, and the muon chanbers, see Fig. 3.2.

The CMS detector is designed to detect the decay products of most of the particles of the SM, except for neutrinos since they are weakly interacting and will almost certainly pass through the entire earth without an interaction. A defining feature of CMS is the 12.6-m long, 5.9 m inner diameter, 3.8 T superconducting solenoid. This is used to bend the trajectory of charged particles thoughout the detector, such that we can reconstruct the momentum and charge of the particles. The LHC provides a 13 TeV proton-proton beam (4.5 TeV heavy ion) beam with a bunch crossing every 25 ns (50 ns) to produce interaction at luminosities of 2.5×10^{34} cm$^{-2}s^{-1}$.

The coordinate system of CMS has the origin at the nominal collision point in the center of the detector. The y-axis points vertically upward, x-axis points radially inward toward the center of the LHC, and z-axis points along the beam directions towards the Jura mountains from LHC Point 5. The polar angle θ is measured from the z-axis and the azimuthal angle ϕ is measured in the $x-y$ plane from the x-axis. The pseudorapidity of a particle is defined as $\eta = -\ln\tan(\theta/2)$ where two notable

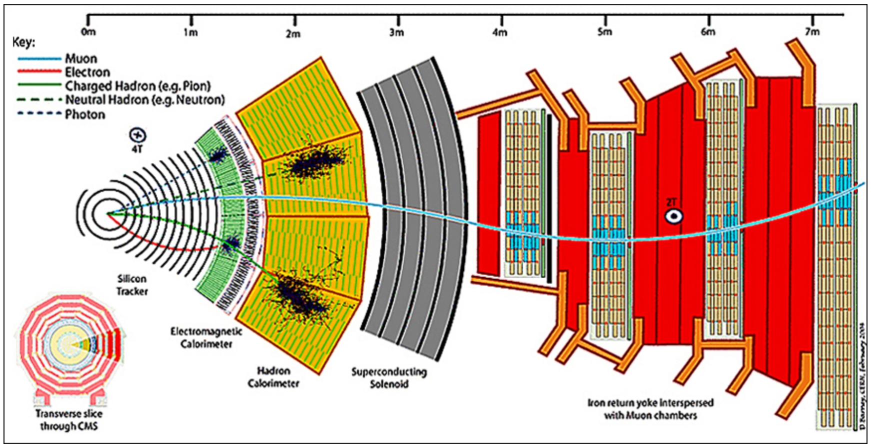

Figure 3.1 : A cross-section of the CMS detector, oriented by looking down the direction of the beam pipe.

values are $\eta = 0$ at $\theta = \pi/2$ and $\eta = \inf$ at $\theta = 0$. The transverse components of momentum, p_T, and energy, E_T, are computed using the x and y components of the particles.

3.2 Silicon Tracker

The silicon tracker is made up of two different detectors, the silicon pixels and the silicon strip tracker. This is the inner most detector for CMS and sees the largest flux of particles during operation. This requires it to be radiation hard and operate with a fine granularity.

3.2.1 Pixel Detector

The pixel detector was recently upgraded during the winter of 2016/2017. It is 1 m long with four barrel layers ranging from 3.0, 6.8, 10.2, and 16.0 cmand three endcap disks. Since it is the closest detector to the interaction vertex it therefore has the highest particle flux at $10^7/\ \text{cm}^2/s$ at $r \equiv 10$ cm. The resolution is 9.4 μm in $r - \phi$ and $20 - 45$ μm in z.

A pixel module contains two layers, a silicon layer and a readout chip that is bump

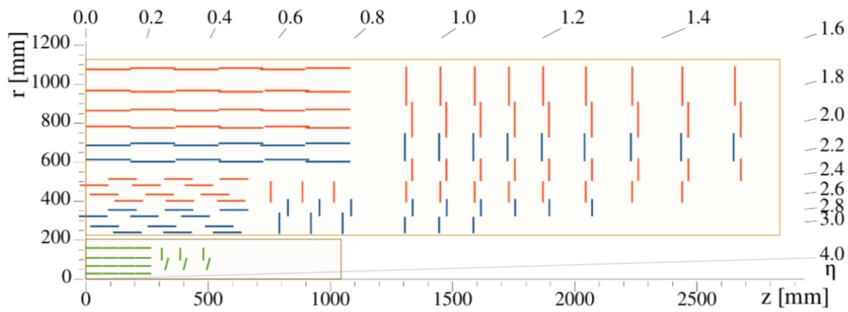

Figure 3.2 : Geometry of the CMS Tracker, the inner most region in green in the pixel detector while the outer region in blue and red are the silicon strips.

bonded to the pixels. The silicon pixel system is set up as a reverse p-n junciton, where the pixels are in the n-type region. As a charged particle travels through the silicon it creates electron-hole pairs. A voltage difference is applied to the silicon such that the electrons will deposit onto the pixels. Since the detector is inside of the magnetic field, a lorentz drift will cause the electrons to reach more than one pixel and increase the resolution. As the pixel system continues to be irradiated with large quantities of particles the voltage in the silicon decreases. This will lead to less charge sharing between the pixels and a decrease in resolution of particle locations. The pixel upgrade has been tested to withstand the expected radiation from collisions until the phase 2 upgrade in 2025.

What is it? Newly installed pixel detector. Larger particle flux and data rate. What is the design of the modules? How do they work? Increased efficiency for b tagging.

3.2.2 Silicon Strips

The silicon strips have a 200 m^2 active region with 15148 modules that are distributed in 10 barrel layers and $9+3$ endcap disks. This has a cell size ranging from 10 cm $\times$ 80 μm to 25 cm $\times$ 180 μm since the particle flux decreases further away from the vertex, [MAYBE ANOTHER FIGURE]. It has a resolution of $23-24$ μm in $r-\phi$

and 23 μm in z for the microstrip tracker

How is it different from the pixels?

3.3 Electromagnetic Calorimeter

The ECAL is a homogeneous calorimeter made out of 61200 lead tungstate ($PbWO_4$) crystals in the barrel and 7324 crystals in each endcap. The barrel region has an inner radius of 129 cm and covers a pseudorapidity range of $0 < |\eta| < 1.479$. The encaps are 314 cm from the interaction point and cover a range $1.479 < |\eta| < 3.0$ in pseudorapidity. Lead tungstate was chosen for teh crystals since it has a short radiation length, $X_0 = 0.89$ cm, fast with 80% of the light being emitted within 25 ns, and it's radiation hard. Each crystal in the barrel has a cross-section of $\approx 22 \times 22\text{mm}^2$ and length of 230 mm, while the endcap crystals are $28.6 \times 28.6\text{mm}^2$ and length of 220 mm corresponding to $25.8X_0$ and $24.7X_0$, respectively. An ECAL uses electromagnetic showers to detect charged particles or photons that interact electromagnetically. Electrons traveling through the material will radiate a photon via bremsstrahlung. A photon will pair produce two electrons. Combining these two processes leads to electromagnetic showers as the particles travel through the detector. The process will continue until a critical energy is reached such that an electron cannot radiate any further and will then lose energy via collisions. The resulting light is recorded by silicon avalanche photodiode (vaccuum phototriodes) in the barrel (endcap).

3.4 Hadronic Calorimeter

The HCAL is a hermetic calorimeter consisting of alternating layers of brass as the absorber material and a scintillator. Brass is chosen since it is non-magnetic and has a relatively short interaction length. In the scintillator, a portion of the energy from the hadron in converted into visible light which is then measured by a hybrid photodiode tube to measure the energy. The barrel part of the HCAL consists of 2304 towers that are segmented into $\Delta\eta \times \Delta\phi = 0.087 \times 0.087$ pieces that cover a region $0 < |\eta| < 1.4$ in pseudorapidity. The encap region consists of 2304 towers with varying segmentation sizes and a coverage of $1.3 < |\eta| < 3.0$.

There are two additional parts of the HCAL to allow for maximum coverage of the detector volume. There is a outer hadron detector that is located outside the superconducting solenoid, which covers a slightly smaller pseudorapidity range as the barrel region. They serve as a tail catcher for hadron showers that penetrate all the way through the inner HCAL and solenoid. A forward hadron calorimeter, located 11.2 m from the interaction point covering a pseudorapidity $3.0 < \eta < 5.0$, made out of steel/quartz fiber is specifically designed for the columnated Cerenkov light in this region.

3.5 Superconducting solenoid

Containing all of this is the superconducting solenoid which is 12.6 m long and a 5.9 m radius. The field strength is 3.8 T which has a stored energy of approximately 2.7 GJ. The magnet is designed such that a muon with momentum, $p = 1$ TeV, will have a momentum resolution of $\Delta p/p \approx 10\%$. The solenoid is a high-purity aluminium-stabilized conductor, which is a similar material used in other large solenoids.

3.6 Muon Chambers

The muon system has three main detection systems that are use to identify a muon candidate. In the barrel region, drift tube (DT) chambers are used since the neutron background, muon rate, and magnetic field are all small. In the endcaps, cathode strip chambers (CSCs) are used since the relative values stated before are much larger. Included throughout the whole system are resistive plate chambers (RPC).

The DT consists on 250 chambers in 4 barrel layers at a radii of 4.0, 4.9, 5.9, and 7.0 m from the beam axis. A DT chamber is an array of anode wires in a gaseous medium where the walls are cathodes. A muon passing through the gas will ionize

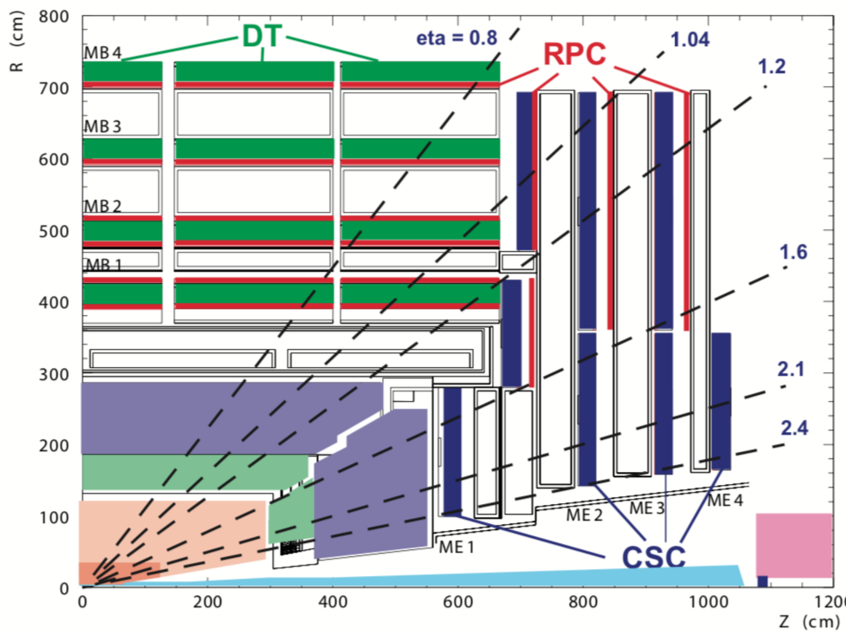

Figure 3.3 : A quarter cross-section of the three detection systems for CMS.

some atoms which are then forced towards the anode wires by an electric field. The drift time of the electrons can then be calculated to within a couple of ns such that a good spatial resolution is achieved. The maximum designed drift length is 2.0 cm. Each station of the DT will give muon vector for each candidate with a ϕ precision of 100 μm in postion and 1 mrad in direction.

The CSC system uses the same concept as the DT system, but also includes a measurement of the ions that follow the electric field to the cathode strips. In this system the anode wires and the cathode strips are perpendicular so the collected charge on both provide a accurate position measurement.

The RPC system contains two parallel plates, anode and cathode, the charge is measured by external metallic strips that can quickly measure the momentum of a muon and decide if the event is worth triggering.

3.7 Physics Objects

There are many different types of physics ojbect that we are interested in when working with particle physics experiments. Since the particles that we are interested in have very short lifetimes, $\mathcal{O}(\text{decay}) = 10^{-23}$ s, we mainly interact with the decay products of the event, such as, jets, heavy object tagging, particle identification, missing transverse energy $\not{E}_T$, H_T, and .

3.8 Jets

In an interaction, because of color confinement, whenever a quark is made it must come in pairs (q, q') such that the total color charge of the interaction in neutral. Typically due to conservation of momentum the quarks may originally be produced near the interaction point but will quickly start to move away from each other. Eventually the quarks will move far enough apart and will have enough potential energy in the gluon connections between them that it is now more efficient to create a new quark-antiquark $(q\overline{q})$ pair. This wil continue to occur in a sequence of radiating gluons and producing new pairs of charged particles. In the final state, the energy deposited in the HCAL is due to a cluster of charged particles of a certain radius, $\Delta R = \sqrt{\Delta\eta^2 + \Delta\phi^2}$. There are many algorithms to reconstruct the jets, we are mainly interested in the anti-k_T method with uses the transverse momentum of the particles within a certain radius $\Delta R = 0.4(0.8)$ for slim(fat) jets.

3.9 Heavy Object Tagging

Since this search is looking for a massive particle which then decays to slightly less massive particles we need to be able to identify and distinguish between them. Firstly, b -tagged jets which are jets that are likely to have originated from a b quark. These are identified reconstructing where the jet originated from and comparing the distance away from the interaction point. A b quark is a relatively long-lived particle and can travel many millimeters before decaying. Since we have a resolution of μm this is not a problem. For b quarks with large transverse momentum, we use a Combined Secondary Vertex (CSVv2/DeepCSV) algorithm depending on the year the data was taken.

Chapter 4

Stop quark Production and Backgrounds

4.1 Production and Decay Modes

Gluon fusion.

Main decay mode mode $\widetilde{t} \rightarrow t + \tilde{\chi}^0_1$, $\widetilde{t} \rightarrow b + \tilde{\chi}^+$. The top quark most likely decays into a b quark and W boson.

4.2 Standard Model Background

Signal events can be mimicked by SM events that have a large number of jets and missing energy.

Broken up into four major backgrounds, Lost Lepton (LL), Znunu, QCD, Rare decays

4.2.1 Lost Lepton

$t\bar{t}$ production of ttbar via the same mechanism as stop-antistop which can be gluon fusion. They then decay the same why as explained above.

W+jets: Production of W bosons plus jets. Jets can be tagged as b jets. W boson decay hadronically or leptonically (where the lepton is missed)

tW and ttW: Missed lepton

4.2.1.1 Transfer Factors

We want to suppress signal contamination by requiring $M_T(l, \not{E}_T) < 100$ GeV. This requirement confirms that it is orthogonal to the search reagions that are used in the search for direct top squark production in the single-lepton final state. Letting the two anaysis statistically combine the results in the future.

We are looking at the event count of data in each corresponding CR for the single-lepton sample. The prediction is allowed by means of a transfer factor (TF) which is obtained from simulation,

$$N_{pred}^{LL} = TF_{LL} \cdot N_{data}(1l). \tag{4.1}$$

This allows us to have the same selection for the single-lepton control sample and the zero-lepton sample. The only exception is the number of top and W-tagged candidates? what is the difference betweeen a candidate and a particle?

The LL estimation is dependent on the yield of data in the corresponding CR and the TF calculated by the single-lepton sample. The transfer factor is defined as,

$$TF_{LL} = \frac{N_{MC}(0l)}{N_{MC}(1l)}, \tag{4.2}$$

where $N_{MC}(1l)$ is the event count observed in the corresponding CR and $N_{MC}(0l)$ use the event count in the corresponding SR.

4.2.2 Z Boson Decay to Neutrinos

Znunu: production of a Z boson that decays into two nuetrinos which are then missed by the detector. Can have jets from other quarks/gluons in the interaction

4.2.3 Quantum Chromodynamic Events

QCD: Events that of jets produced by QCD processes. The missing energy from from a mismeasurement of the jets in the event causing missing energy

4.2.4 Rare Interactions

ttZ, ttH, WW, WZ, ZZ, tZq, tWZ: rare processed that can have jets plus MET. Expand upon these later

Chapter 5

Search Region Design

Using MC simulations that model the SM background for this process we want to reduce the number of events in our Search region. This is an all hadronic search so we are looking at event with zero tagged leptons. Unfortunately, some can get in by not passing the kinematic cuts or just by the non 100 % of the detector. There is a small nonzero inefficiency of mistagging a lepton as something else.

5.1 Minimizing the ttZ background

For the ttZ interactions, we produce two top quarks that can then decay to two b quarks and two W bosons. A possible way to mimick our search region is two have multiple jets, i.e. b quarks that hadronize and W bosons that decay hadronically, but we also need missing energy. This will be in addition to the Z boson decaying into two neutrinos and thus creating a large amount of missing energy.

We now try to look at the differing kinematic structure of the background, ttZ, and the signal region, stop quarks decaying. Under the assumption that the Z boson is created by radiated from the top quark the resulting decay to neutrinos should be close, small $\Delta\phi$, between the resulting jets. For the signal, the missing energy is produced by the neutralino. When the stop quark decays into top quark and neutralino the top quark should recoil off of neutralino to essentially be back-to-back. This will cause a large angle, $\Delta\phi$, between them. We then want to use the kinematic variable, $\Delta\phi(t_{1,2}, \not{E}_T)$, where

5.2 Lost Lepton Application

Can we apply this to other backgrounds. For boosted tops the the missing energy caused by missing the lepton in the W boson decay. The variable $\Delta\phi(t_{1,2}, \not{E}_T)$should also apply. Should work for wjts, tW, ttW.

5.3 Search Regions

The HM and LM Search regions should be defined and explained. Why are they defined the way they are?

5.4 Search Region Optimization

Look for an optimized cust for $\Delta\phi(t_{1,2}, \not{E}_T)$to maximize $\frac{S}{\sqrt{B}}$ in each SR. Could have a different cut for each region, but a combination to make it all the same would be nice. Since the signal can decay in multiple ways we need to optimize for all possible scenarios. Explain why we are maximizing $\frac{S}{\sqrt{B}}$

5.5 Limits

Looking at the significance and limits for the mass regions of the stop quark decay. Using the Higgs Combined tool, which includes statistics with a ”maximal likelihood” fit? The cut, $\Delta\phi(t_{1,2}, \not{E}_T)$, would hopefully improve the values, but an optimized cut has not been chosen yet.